THE JOURNAL OF BIOLOGICAL CHEMISTRY
Vol. 279, No. 20, Issue of May 14, pp. 21046–21054, 2004

Printed in U.S.A.

Structure and Biological Activity of the Short-chain Lipopolysaccharide from *Bartonella henselae* ATCC 49882^T*

Received for publication, December 8, 2003, and in revised form, January 26, 2004
Published, JBC Papers in Press, February 7, 2004, DOI 10.1074/jbc.M313370200

Ulrich Zähringer‡§, Buko Lindner‡, Yuriy A. Knirel‡, Willem M. R. van den Akker¶, Rosemarie Hiestand‖, Holger Heine‡, and Christoph Dehio‖

From the ‡Research Center Borstel, Leibniz-Center for Medicine and Biosciences, 23845 Borstel, Germany, the ¶Hubrecht Laboratory, Netherlands Institute for Developmental Biology, 3584 CT Utrecht, The Netherlands, and the ‖Biozentrum of the University of Basel, Division of Molecular Microbiology, 4056 Basel, Switzerland

The facultative intracellular pathogen *Bartonella henselae* is responsible for a broad range of clinical manifestations, including the formation of vascular tumors as a result of increased proliferation and survival of colonized endothelial cells. This remarkable interaction with endotoxin-sensitive endothelial cells and the apparent lack of septic shock are considered to be due to a reduced endotoxic activity of the *B. henselae* lipopolysaccharide. Here, we show that *B. henselae* ATCC 49882^T produces a deep-rough-type lipopolysaccharide devoid of *O*-chain and report on its complete structure and Toll-like receptor-dependent biological activity. The major short-chain lipopolysaccharide was studied by chemical analyses, electrospray ionization, and matrix-assisted laser desorption/ionization mass spectrometry, as well as by NMR spectroscopy after alkaline deacylation. The carbohydrate portion of the lipopolysaccharide consists of a branched trisaccharide containing a glucose residue attached to position 5 of an α-(2→4)-linked 3-deoxy-D-*manno*-oct-2-ulosonic acid disaccharide. Lipid A is a pentaacylated β-(1′→6)-linked 2,3-diamino-2,3-dideoxyglucose disaccharide 1,4′-bisphosphate with two amide-linked residues each of 3-hydroxydodecanoic and 3-hydroxyhexadecanoic acids and one residue of either 25-hydroxyhexacosanoic or 27-hydroxyoctacosanoic acid that is *O*-linked to the acyl group at position 2′. The lipopolysaccharide studied activated Toll-like receptor 4 signaling only to a low extent (1,000–10,000-fold lower compared with that of *Salmonella enterica* sv. Friedenau) and did not activate Toll-like receptor 2. Some unusual structural features of the *B. henselae* lipopolysaccharide, including the presence of a long-chain fatty acid, which are shared by the lipopolysaccharides of other bacteria causing chronic intracellular infections (*e.g. Legionella* and *Chlamydia*), may provide the molecular basis for low endotoxic potency.

Bartonella henselae is an emerging zoonotic pathogen. In the feline reservoir host this cat flea-borne Gram-negative pathogen causes a long lasting intraerythrocytic bacteremia associated with little or no symptoms of disease (1). *B. henselae* is transmitted to humans by cat scratch or bite or the bite of an infected cat flea. Human infection results in a broad range of clinical manifestations, which often have a chronic course. Cat-scratch disease is a necrotizing inflammatory lymphadenitis typically associated with fever, which represents the most common disease manifestation in immunocompetent patients. Prolonged febrile bacteremic syndrome is a frequent disease manifestation of immunocompromized patients, which, unlike bacteremia by most other Gram-negative bacteria, has never been reported to result in septic shock. Bacillary angiomatosis and bacillary peliosis are angioproliferative lesions also found primarily in immunocompromised hosts (2).

Angioproliferation stimulated by *B. henselae* is a remarkable pathogenic process which represents a unique model to study pathogen-triggered tumor formation. Judged from the histology of bacillary angiomatosis and bacillary peliosis lesions, bacteria are in direct contact with the endothelium, probably triggering both endothelial cell proliferation and proinflammatory activation. Therefore, endothelial cells appear to represent a specific and unique target of *B. henselae*, and a detailed analysis of the bacteria-endothelial cell interactions is thus vital for understanding the pathophysiology of this emerging infection. Human umbilical vein endothelial cells have been used as an *in vitro* model to study important steps in the interaction of *B. henselae* with endothelial cells. This facultative intracellular pathogen invades endothelial cells by two different processes, either (i) by conventional endocytosis of single bacteria or small bacterial aggregates, which results in perinuclear-localizing intravacuolar bacteria, or (ii) by the invasion of large bacterial aggregates by a host cell-driven process referred to as invasome-mediated internalization (3).

B. henselae is considered to provoke angioproliferation by at least two independent mechanisms (4): directly, by triggering proliferation (5) and inhibiting apoptosis of endothelial cells (6) and indirectly, by stimulating a paracrine angiogenic loop of vascular endothelial growth factor production by infected macrophages (7).

The lipopolysaccharides (LPS)[1] of Gram-negative bacteria are known as endotoxins, which cause the prominent patho-

* This work was supported by Deutsche Forschungsgemeinschaft Grants LI-448/1-1 (to B. L. and U. Z.) and ZA 149/3-2 (to U. Z.) and by Swiss National Science Foundation Grant 31-61777.00 (to C. D.). The costs of publication of this article were defrayed in part by the payment of page charges. This article must therefore be hereby marked "*advertisement*" in accordance with 18 U.S.C. Section 1734 solely to indicate this fact.

§ To whom correspondence should be addressed. Tel.: 49-4537-188462; Fax: 49-4537-188406; E-mail: uzaehr@fz-borstel.de.

[1] The abbreviations used are: LPS, lipopolysaccharide; COSY, correlation spectroscopy; ESI, electrospray ionization; FT-ICR, Fourier transform ion cyclotron resonance; GLC, gas-liquid chromatography; Glc, D-glucose; GlcN, D-glucosamine; GlcN3N, 2,3-diamino-2,3-dideoxyglucose; HMQC, heteronuclear multiple-quantum coherence; HPAEC, high-performance anion-exchange chromatography; IRMPD, infrared multiphoton dissociation; Kdo, 3-deoxy-D-*manno*-oct-2-ulosonic acid; MALDI-TOF, matrix-assisted laser desorption/ionization time-of-flight; MS, mass spectrometry; ROESY, rotating-frame nuclear Overhauser effect spectroscopy; TOCSY, total correlation spectroscopy; 12:0(3-OH), 12:1(3-OH), 16:0(3-OH), 26:0(25-OH), 28:0(27-OH), etc., 3-hydroxydodecanoic, 3-hydroxydodecenoic, 3-hydroxyhexadecanoic, 25-hydroxyhexacosanoic, 27-hydroxyoctacosanoic acids, etc.

physiological symptoms associated with sepsis and septic shock, *i.e.* fever, leukopenia, hypertension, disseminated intravascular organ failure, and multiple organ failure. The LPS from enteric bacteria, such as *Escherichia coli* and *Salmonella enterica*, are highly potent molecules with regard to their biological, *i.e.* endotoxic activities. The lipid A portion is responsible for these activities of the enterobacterial LPS (8). Endothelial cells sense the endotoxin by soluble CD14 and toll-like receptor 4 (TLR4), resulting in the nuclear factor κB (NF-κB)-dependent activation of a proinflammatory response. This phenotype is characterized by the up-regulation of the adhesion molecules ICAM-1 and E-selectin and the secretion of proinflammatory cytokines and chemokines (9).

B. henselae infection of human umbilical vein endothelial cells results in a prominant NF-κB-dependent proinflammatory activation (10, 11). However, this process is triggered by proteinacious components of the bacteria rather than by LPS (10). A mutant defective for the bacterial type IV secretion system VirB was shown to display only minimal activation of NF-κB, suggesting that bacterial effector proteins translocated by this system into endothelial cells are responsible for the proinflammatory phenotype observed during infection with wild-type *B. henselae* (11). Moreover, in contrast to wild type, the VirB-defective mutant displayed any noticeable toxic effect on endothelial cells, even at very high infection doses (11). Assuming that LPS is not affected in the VirB-defective mutant, the LPS of *B. henselae* appears to be devoid of toxicity for endothelial cells (11). This observation together with the apparent absence of septic shock in bacteremic patients indicates that the LPS of this pathogen is of low endotoxic activity. The *B. henselae* LPS should thus be interesting in regard to structure/function analysis. This LPS is composed of a major rough-type form (R-form, lacking *O*-chain), and a minor smooth-type form (S-form, containing *O*-chain) (12). However, despite the presence of a long-chain fatty acid (13), no information is available regarding the structure of *B. henselae* LPS and lipid A. Based on the limited information available, a simliar LPS is found in the closely related species *B. bacilliformis* and *B. quintana*, which represent the only other known pathogens capable of triggering angioproliferative lesions in humans. The *B. bacilliformis* LPS is also composed of a minor S-form and a major R-form, the latter being poorly immunogenic in rabbits (14). Consistently, the *B. quintana* LPS was described to be predominantly of a "deep-rough" chemotype (15) and was further shown to possess a lower endotoxic activity on whole blood cells and endothelial cells than typical endotoxins (15, 16).

In this paper, we describe elucidation of the structure of a short-chain LPS representing the major LPS species from *B. henselae* ATCC 49882^T. The unusual structural features of this novel LPS are: (i) pentaacyl lipid A, containing a GlcN3N disaccharide bisphosphate [4′-*P*-β-D-Glc*p*N3N-(1→6)-α-D-Glc*p*N3N-1→*P*] as the lipid A backbone and a long-chain fatty acid, namely 26:0(25-OH) or 28:0(27-OH), and (ii) a small and unique inner core composed of an α-(2→4)-linked 3-deoxy-d-*manno*-oct-2-ulosonic acid (Kdo) disaccharide with one glucose residue attached. Moreover, we demonstrated that this LPS has a low endotoxic potential as measured by TLR4 signaling and, in contrast to LPS from some other pathogens, does not activate TLR2-signaling to any considerable extend. The structure and biological activity of the *B. henselae* ATCC 49882^T short-chain LPS displays interesting parallels with LPS of rhizobacteria, which are phylogenetically related intracellular plant symbionts, as well as with some human pathogens poorly related to *B. hensleae* (*e.g. Legionella* and *Chlamydia*), which, however, share the intracellular life style and the typical chronic course of infection.

EXPERIMENTAL PROCEDURES

Bacterial Strains and Cultivation—*B. henselae* ATCC 49882^T isolated from the blood of an human immunodeficiency virus-positive febrile patient was obtained from the Collection de l'Institut Pasteur (CIP), Paris, France. *B. henselae* IBS 113 isolated from the blood of a bacteremic cat was kindly provided by Dr. Y. Piemont, Hopital Louis Pasteur, University of Strasbourg, Strasbourg, France. *B. henselae* ATCC 49882^T was grown for 3 days on Columbia agar containing 5% defibrinated sheep blood at 35 °C in a humidified atmosphere.

Small Scale Isolation of LPS for SDS-PAGE—Bacterial LPS was isolated from proteinase K-treated whole bacteria, separated by Tricine-SDS-PAGE and stained by oxidative silver staining as previously described for *Bordetella* spp. (17).

Preparative Isolation of LPS—Bacteria were harvested from 500 plates in phosphate-buffered saline and washed twice in distilled water, followed each time by centrifugation for 30 min at 18,000 × *g*. The bacterial pellet was finally suspended in a small volume of aqueous 0.5% phenol. Dried bacteria (3.1 g) were washed successively with ethanol (300 ml), acetone (300 ml), and diethyl ether (300 ml) and dried in air overnight. The pellet was suspended in water (250 ml), treated first with RNase and DNase (2 mg each) at stirring over night at room temperature, then with proteinase K (2 mg) for 24 h at 20 °C, dialyzed extensively (4 days) against distilled water, and centrifuged. The precipitate was washed with acetone, suspended in water, and lyophilized (final yield of washed bacteria: 1.63 g).

Attempts to isolate LPS by direct extraction of the digested dried bacterial cells described above using the phenol-water (P/W) (18) or phenol/chloroform/petrol ether procedures (19) were not satisfactory. After extensive enzyme digestions using proteinase K in the presence of SDS, mercaptoethanol, and lysozyme, sufficient quantities of *B. henselae* LPS for analytical studies could be extracted by the phenol/chloroform/petrol ether (2:5:8, v/v/v) procedure (19). To remove non-LPS lipids, prior to extraction cells were washed three times with a 1:1 (v/v) chloroform/methanol mixture, centrifuged, and dried in a stream of nitrogen. To remove residual protein from this crude LPS perparation, the protocol of Hirschfeld *et al.* (20) was used. An aliquot of the extract containing 5 mg of LPS gave 2.9 mg of purified LPS, which showed no banding pattern in SDS-PAGE and Coomassie Brilliant Blue staining.

O-Deacylation of LPS—LPS (14 mg) was dried over P_2O_5 and treated with anhydrous hydrazine (0.5 ml) at 37 °C for 35 min at ultrasonication. Acetone (5 ml) was added in the cold and the precipitate was separated by centrifugation, washed twice with acetone, dissolved in water (3 ml), and lyophilized. The product was treated with anhydrous hydrazine at 37 °C for 1.5 h and treated as above to give O-deacylated LPS (11 mg).

Alkaline Degradation of LPS—*O*-Deacylated LPS (11 mg) was heated with 4 M KOH (1 ml) at 120 °C for 23.5 h, and the reaction mixture was diluted with water (5 ml), neutralized at 0 °C with 2 M HCl (2 ml), and extracted with chloroform (2 × 4 ml). After separation of phases the precipitate was washed with water (2 × 2 ml), the combined water phase and washings were lyophilized. The product was desalted by gel chromatography on Sephadex G-50 in pyridinium acetate buffer, pH 4.5 (4 ml of pyridine and 10 ml of HOAc in 1 liter of water), and fractionated by HPAEC using a Dionex system with pulsed amperometric detection on an analytical CarboPac PA1 column (250 × 4.6 mm) in a linear gradient of 0.15 → 0.5 M NaOAc in 0.1 M NaOH for 70 min at 1 ml/min. 1-ml fractions were collected and analyzed by HPAEC using the same gradient for 30 min at 1 ml/min. Four products with retention times 19.25, 21.35, 24.75 (major, 300 μg), and 28.10 min in the analytical run were isolated and desalted on a column (40 × 2.5 cm) of Sephadex G-50 in pyridinium acetate buffer, pH 4.5.

Mild Acid Degradation of LPS—LPS (0.4 mg) was hydrolyzed with 0.1 M sodium acetate buffer, pH 4.4, at 100 °C for 2 h, and the supernatant was deionized with an IR-120 (H^+-form) cation-exchange resin and analyzed by HPAEC in a linear gradient of 0.01 → 0.08 M NaOAc in 0.1 M NaOH for 30 min at 1 ml/min, which showed the presence of two compounds with retention times of 23.38 and 24.55 min.

Composition Analyses—For analysis of Kdo, LPS was methanolyzed with 0.5 M HCl in methanol at 85 °C for 45 min. After removal of the solvent, the products were peracetylated with Ac_2O in pyridine (1:1.5, v/v, 85 °C, 20 min). For analysis of Glc and GlcN3N, LPS was methanolyzed with 2 M HCl in methanol at 85 °C for 16 h, then hydrolyzed with 4 M CF_3CO_2H at 100 °C for 2 h, conventionally borohydride-reduced and peracetylated (21). For fatty acid analysis, LPS was methanolyzed with 2 M HCl in methanol at 85 °C for 20 h, and sugars were trimethylsilylated with *N*,*O*-bis(trimethylsilyl)trifluoroacetamide (22). The sugar and fatty acid derivatives were analyzed by GLC on a

Hewlett-Packard HP 5890 Series II chromatograph, equipped with a 30-m fused silica SPB-5 column (Supelco) using a temperature gradient of 150 °C (3 min) → 320 °C at 5°/min, and GLC-MS on a Hewlett-Packard HP 5989A instrument equipped with a 30-m HP-5MS column (Hewlett-Packard) under the same chromatographic conditions as in GLC.

Methylation Analysis—*O*-Deacylated LPS was dephosphorylated with aqueous 48% hydrofluoric acid (4 °C, 16 h), methylated with CH_3I in dimethyl sulfoxide in the presence of solid NaOH (23), and hydrolyzed with 2 M CF_3CO_2H (100 °C, 2 h). The partially methylated monosaccharides were borohydride-reduced, and Kdo was converted into the methyl ester by evaporation with 0.5 M HCl in methanol, peracetylated, borohydride reduced, peracetylated, and analyzed by GLC and GLC-MS as described above.

Mass Spectrometry—MALDI-TOF MS was performed on a Bruker-Reflex II instrument (Bruker-Franzen Analytik, Bremen, Germany) in linear configuration in the negative mode at an acceleration voltage of 20 kV and delayed ion extraction. Samples were dissolved in chloroform at a concentration of 5 μg/μl, and 2 μl of solution was mixed with 2 μl of 0.5 M 2,4,6-trihydroxyacetophenone (Aldrich) in methanol as matrix solution. 1-μl aliquots were deposited on a metallic sample holder and analyzed immediately after drying in a stream of air.

ESI FT-ICR MS/MS was performed using a Fourier transform ion cyclotron resonance mass analyzer (ApexII, Bruker Daltonics) equipped with a 7-tesla actively shielded magnet and an Apollo electrospray ion source. Samples were dissolved in a 30:30:0.01 (v/v/v) mixture of 2-propanol, water, and triethylamine at a concentration of ~20 ng/μl and sprayed with a flow rate of 2 μl/min. For IRMPD MS/MS, a 40-watt CO_2 laser (Synrad Inc., Mukilteo, WA) operating at λ = 10.6 μm was used. Laser power was set to 50% of maximal value. Duration of irradiation was controlled via the XMASS software (Bruker Daltonics) for optimal fragmentation (typically 50 ms).

NMR Spectroscopy—Prior to the measurements, the samples were lyophilized twice from ^2H_2O. The ^1H and ^{31}P NMR spectra were recorded with a Bruker DRX-600 spectrometer (Bruker, Rheinstetten, Germany) at 600 and 243 MHz, respectively, at 27 °C in 99.96% ^2H_2O. Chemical shifts were referenced to internal sodium 3-trimethylsilylpropanoate-d_4 (δ_H 0) and external aqueous 85% H_3PO_4 (δ_P 0). Bruker software XWINNMR 2.5 was used to acquire and process the data. A mixing time of 100 and 200 ms was used in two-dimensional TOCSY and ROESY experiments, respectively.

Activation of HEK/HEK-CD14 Cells—For transient transfection, HEK293 cells were plated at a density of $5{\cdot}10^4$/ml in 96-well plates in Dulbecocc's modified Eagle's medium without G418. The following day, cells were transfected using Polyfect (Qiagen) according to the manufacturer's protocol. Expression plasmid containing human CD14 was a kind gift of Dr. D. T. Golenbock, Worcester, MA, and the FLAG-tagged versions of human TLR2 and human TLR4 were a kind gift from P. Nelson, Seattle, WA and subcloned into pREP9 (Invitrogen). The human MD-2 expression plasmid was a kind gift from K. Miyake, Tokyo, Japan. TLR2 and TLR4 plasmids were used at 200 ng/transfection, CD14 and MD-2 plasmids were used at 25 ng/transfection. The total DNA content was kept constant at 250 ng/transfection using pCDNA3 (Invitrogen). After 24 h of transfection, cells were washed and stimulated with LPS for another 18 h. Finally, supernatants were collected and the interleukin-8 content was quantified using a commercial enzyme-linked immunosorbent assay (BIOSOURCE).

Bacterial lipopeptide ($Pam_3CysSK4$) was obtained from EMC microcollections, Tübingen, Germany, and LPS from *S. enterica* sv. Friedenau was kindly provided by H. Brade, Borstel, Germany.

RESULTS

Purification of B. henselae LPS and Analysis by SDS-PAGE—Crude LPS extracts from *B. henselae* isolated following proteinase K treatment of whole cells was separated by SDS-PAGE and visualized by silver staining. Consistent with a recent study examining the LPS composition of several *B. henselae* strains (12), we observed for strains ATCC 49882^T (Fig. 1*A*, *lane 1*) and IBS 113 (*lane 2*) the presence of at least two LPS species of different electrophoretic mobility, an R-form of about 3 kDa as the major constituent and at least one S-form of >20 kDa as a minor constituent. LPS was then isolated in preparative scale from cells of *B. henselae* ATCC 49882^T by phenol/chloroform/petrol ether extraction (19) following extensive digestion of bacterial cells with proteolytic enzymes. Extraction with chloroform/methanol was necessary to remove non-LPS lipids. When this purified LPS was tested, no high molecular mass S-form LPS was observed (Fig. 1*B*, *lane 1*), indicating selective enrichment of the R-form during phenol/chloroform/petrol ether extraction. The mobility of the R-form LPS was in the range between that of *E. coli* deep-rough mutant strain F515 (chemotype Re, containing two Kdo residues as the core oligosaccharide; Fig. 1*B*, *lane 2*) and *S. enterica* sv. Minnesota rough mutant R7 (chemotype Rd_1, containing two Kdo and two heptose residues; Fig. 1*B*, *lane 3*). Therefore, *B. henselae* ATCC 49882^T produces a short-chain R-form LPS with a core ranged in size between di- and tetrasaccharide.

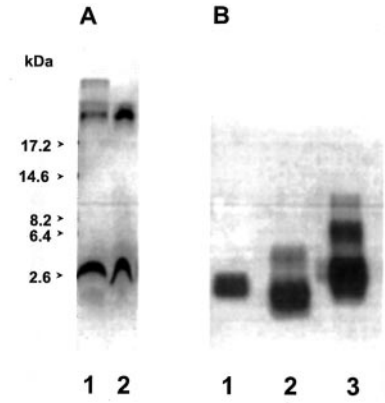

FIG. 1. **Silver-stained SDS-PAGE (20%).** *A*, small scale isolation of LPS from *B. henselae* ATCC 49882^T (*lane 1*) and strain IBS 113 (*lane 2*). *B*, purified LPS from *B. henselae* ATCC 49882^T (*lane 1*), *E. coli* mutant F515 (chemotype Re, *lane 2*), and *S. enterica* sv. Minnesota mutant R7 (chemotype Rd_1, *lane 3*).

Chemical and Mass Spectrometric Characteriztaion of LPS—Sugar analysis of the purified LPS showed the presence of Glc, Kdo, and GlcN3N, but no GlcN. Most likely, Glc and Kdo are components of the core oligosaccharide portion of LPS, whereas GlcN3N has been previously identified in the lipid A backbone of several bacteria (24). Fatty acid analysis revealed 12:0(3-OH), 16:0(3-OH), 26:0(25-OH), and 28:0(27-OH) as the major constituents, together with 12:1(3-OH), 14:0(3-OH), 18:0(3-OH) as minor constituents, and a negligible amount of 18:1(3-OH).

Methylation analysis of the *O*-deacylated dephosphorylated LPS, including carboxyl reduction of Kdo, demonstrated 4,5-disubstituted Kdo (Kdo^I), terminal Glc, and terminal Kdo (Kdo^{II}). These data indicated that the LPS core is a branched trisaccharide composed of one Glc and two Kdo residues. A minor amount of a 5-substituted Kdo residue was also detected, which, most likely, resulted from a partial elimination of the terminal Kdo residue in the course of dephosphorylation of LPS under acidic conditions (25).

The charge-deconvoluted negative ion ESI FT-ICR mass spectrum of LPS (Fig. 2) showed two major molecular ion peaks at *m/z* 2399.44 (M^I) and 2427.45 (M^{II}) and a minor peak at *m/z* 2455.50. Taking into account the composition of LPS, the major peaks could be assigned to LPS species containing a $GlcKdo_2$ trisaccharide and a bisphosphoryl di-GlcN3N lipid A backbone acylated with two residues each of 12:0(3-OH) and 16:0(3-OH) and one residue of either 26:0(25-OH) or 28:0(27-OH). The minor compound may differ in the replacement of one 12:0(3-OH) or 16:0(3-OH) residue with a residue of 14:0(3-OH) or 18:0(3-OH), respectively. Furthermore, the spectrum exhibited minor peaks representing compounds missing one phosphate group (*m/z* 2319.47, 2347.50, and 2365.51) or those containing one unsaturated fatty acid (*m/z* 2397.43, 2425.45, and 2453.50). Unlabelled peaks in Fig. 2 represent sodium adduct ions.

Positive ion ESI FT-ICR IRMPD MS/MS of triethylammo-

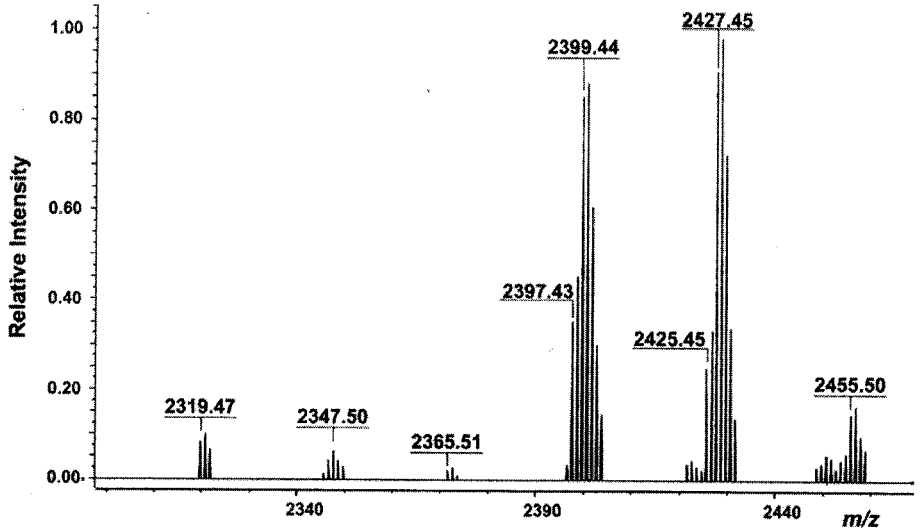

FIG. 2. **Charge-deconvoluted negative ion FT-ICR ESI mass spectrum of LPS of *B. henselae* ATCC 49882^T.**

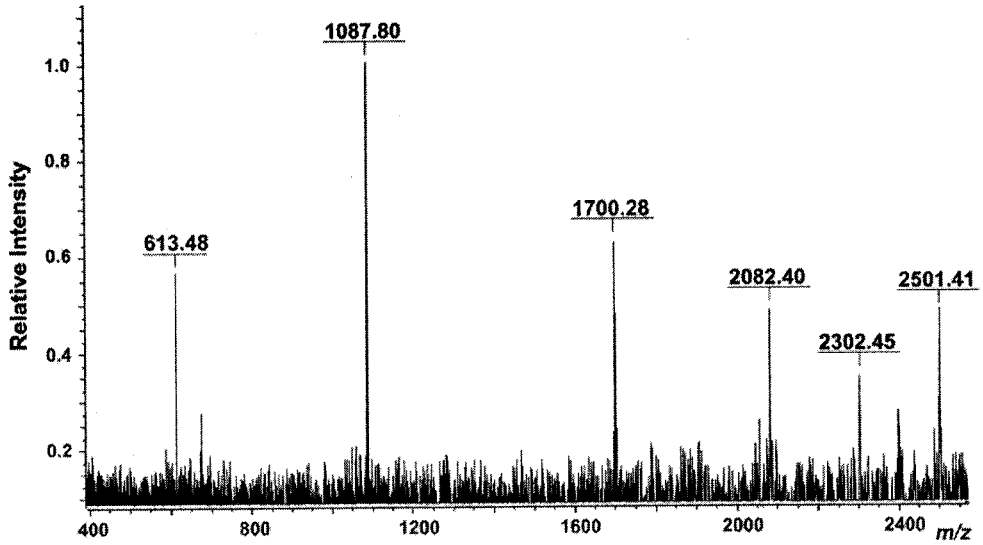

FIG. 3. **Positive ion ESI FT-ICR IRMPD MS/MS of triethylammonium salt of LPS of *B. henselae* ATCC 49882^T.** The molecular ion at *m/z* 2501.41 was used as the parent ion.

nium salt of LPS was performed using the molecular ion at *m/z* at 2501.41 (M^I-salt) as the parent ion (Fig. 3). The spectrum showed ion peaks due to subsequent loss of triethylammonium phosphate (*m/z* 2302.45) and Kdo (*m/z* 2082.40) or the $GlcKdo_2$ trisaccharide (*m/z* 1700.28, lipid A ion). The monophosphoryl lipid A ion was further cleaved to give β- and γ-fragment ions (according to the nomenclature of Domon and Costello) at *m/z* 1087.80 and an ion from the reducing end at *m/z* 613.48 (711.48, *P*), respectively. This fragmentation pattern showed that each GlN3N residue in lipid A bears one 12:0(3-OH), one 16:0(3-OH), and one phosphate group and that in M^I the 26:0(25-OH) residue is attached to the non-reducing GlcN3N residue ($GlcN3N^{II}$).

Alkaline Degradation of LPS and Structure of the Carbohydrate Core-Lipid A Backbone—LPS was *O*-deacylated with anhydrous hydrazine. As expected, the negative ion ESI FT-ICR mass spectrum of the *O*-deacylated LPS showed ion peaks at *m/z* 2005.04 (major) and 2033.08 (minor) for LPS species with four *N*-linked fatty acids. Further *N*-deacylation of the *O*-deacylated LPS resulted in a mixture of four oligosaccharide bisphosphates, which were separated by HPAEC. In negative ion ESI FT-ICR MS/MS, the major compound (*1*) with the HPAEC retention time 24.75 min showed a molecular ion peak at *m/z* 1099.28 and thus has the full core trisaccharide. The other compounds have a truncated core lacking either Kdo^{II} or Glc or both Kdo^{II} and Glc (molecular ions at *m/z* 879.22, 937.22, and 717.17, respectively) (data not shown). The content of the Kdo^{II}-lacking product with the retention time 19.25 min was twice as low as that of the major compound, whereas the two Glc-lacking products were present in negligible amounts. Since no compound with a truncated core was detected in MS studies on the whole LPS, the minor compounds resulted from partial cleavage of the glycosidic linkages under strong alkaline conditions.

Compound 1 was studied by high-field NMR spectroscopy. The ^1H NMR spectrum of compound 1 (Fig. 4) showed signals for three anomeric protons at δ 4.32, 5.22, and 5.26, protons at nitrogen-bearing carbons (H-2 and H-3) of two GlcN3N residues at δ 2.48, 2.55, 2.61, and 2.82, and methylene groups of two Kdo residues at δ 1.72, 1.92 (both H-3ax), 2.02, and 2.05 (both H-3eq). The spectrum was completely assigned using two-dimensional $^1H,^1H$ COSY, TOCSY, and $^1H,^{13}C$ HMQC ex-

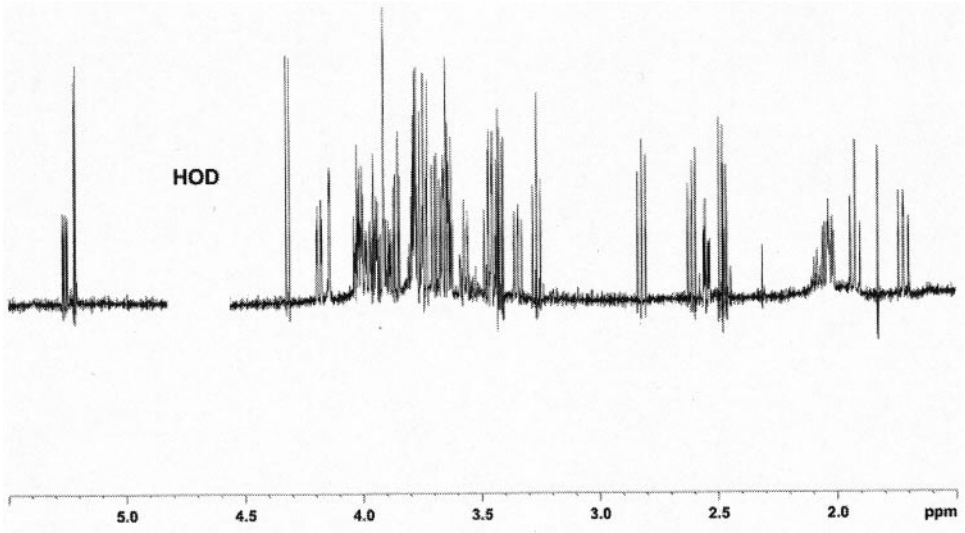

FIG. 4. **^{1}H NMR spectrum of the compound 1 isolated from LPS of *B. henselae* ATCC 49882^T by stepwise *O*- and *N*-deacylation.** For signal assignment, see Table I.

TABLE I
^{1}H NMR chemical shifts of the compound 1 from LPS of B. henselae ATCC 49882^T

Sugar residue	H-1H-3ax	H-2H-3eq	H-3H-4	H-4H-5	H-5H-6	H-6aH-7	H-6bH-8a	H-8b
α-Glc*p*-(1→	5.22	3.42	3.74	3.46	4.01	3.78	3.78	
α-Kdo*p*^{II}-(2→	1.72	2.05	3.90	3.90	3.64	3.96	3.65	3.78
→4,5)-α-Kdo*p*^{I}-(2→	1.92	2.02	4.02	4.14	3.68	3.94	3.69	3.85
→6)-β-Glc*p*N3N4*P*^{II}-(1→	4.32	2.48	2.61	3.45	3.57	3.34	3.74	
→6)-α-Glc*p*N3N^{I}-1-*P*	5.26	2.55	2.82	3.26	3.99	3.64	4.18	

TABLE II
^{13}C NMR chemical shifts of the compound 1 from LPS of B. henselae ATCC 49882^T

Chemical shifts were determined from the two-dimensional ^{1}H,^{13}C HMQC spectrum.

Sugar residue	C-1	C-2	C-3	C-4	C-5	C-6	C-7	C-8
α-Glc*p*-(1→	100.8	73.5	73.9	70.5	72.9	61.4		
α-Kdo*p*^{II}-(2→			36.1	68.0[a]	68.0[a]	73.6[a]	70.4	64.5
→4,5)-α-Kdo*p*^{I}-(2→			36.0	73.1	75.1	73.3	72.0	64.0
→6)-β-Glc*p*N3N4*P*^{II}-(1→	105.2	57.5	59.6	75.3	77.5	64.7		
→6)-α-Glc*p*N3N^{I}-1-*P*	95.7	56.7	55.0	71.5	72.8	70.8		

[a] Superposition of two non-resolved signals.

periments, and spin systems of one Glc, two GlcN3N, and two Kdo residues were identified. The ^{1}H and ^{13}C NMR chemical shifts (Tables I and II) and typical coupling constant values indicated that all sugar residues are in the pyranose form. A large $J_{1,2}$ coupling constant of 8.0 Hz for the H-1 signal at δ 4.32 showed that one of the GlcN3N residues (GlcN3N^{II}) is β-linked, whereas Glc and GlcN3N^{I} are α-linked ($J_{1,2}$ 3.5 and 3.3 Hz for the H-1 signals at δ 5.22 and 5.26, respectively). The H-1 signal of α-GlcN3N^{I} was additionally split due to coupling to phosphorus ($J_{1,P}$ 8.6 Hz). The α-configuration of both Kdo residues followed from the characteristic ^{1}H and ^{13}C NMR chemical shifts, which were similar to those of α-Kdo*p* but different from the values of β-Kdo*p* (26).

A two-dimensional ROESY experiment revealed correlations of the anomeric proton of GlcN3N^{II} with the protons at the linkage carbon H-6a,6b of GlcN3N^{I} at δ 4.32/3.64 (strong) and δ 4.32/4.18 (weak), thus indicating the β1→6-linkage between the monosaccharides in the lipid A backbone. As expected, no interresidue cross-peak was observed for H-1 of GlcN3N^{I} at δ 5.26. The anomeric proton of Glc showed correlations with H-5 and H-7 of Kdo^{I} at δ 5.22/4.14 (strong) and 5.22/3.94 (weak), respectively, which are typical of the α1→5-linkage between these sugar residues (27). Finally, a strong correlation between H-3eq of Kdo^{I} and H-6 of Kdo^{II} at δ 2.02/3.64 proved that Kdo^{I} and Kdo^{II} are α-(2→4)-interlinked (27, 28).

The glycosylation pattern was further confirmed by the ^{13}C NMR chemical shift data of the linkage carbons (Table II), whose signals typically shifted down-field compared with their positions in the corresponding non-substituted monosaccharides. The displacements were relatively large when the substituent is an aldopyranose (7–8 ppm for C-5 of Kdo^{I} and C-6 of GlcN3N^{I} caused by glycosylation with Glc and GlcN3N^{II}, respectively) and smaller in case of a ketopyranose substituent (~5 and ~2 ppm for C-4 of Kdo^{I} and C-6 of GlcN3N^{II} glycosylated with Kdo^{II} and Kdo^{I}, respectively).

The ^{31}P NMR spectrum of compound 1 contained signals for two phosphate groups at δ 4.72 and 4.94. A ^{1}H,^{31}P HMQC experiment showed correlations of the former with H-1 of GlcN3N^{I} at δ_P/δ_H 4.72/5.26 and the latter with H-4 of GlcN3N^{II} at δ_P/δ_H 4.94/3.45. Therefore, the lipid A disaccharide backbone is bisphosphorylated at positions 1 and 4′, and the compound 1 has the structure shown in Fig. 5.

Mild Acid Degradation and Full Structure of LPS—Hydrolysis of LPS at pH 4.4 cleaved the Kdo linkages, including the linkage between Kdo^{I} and lipid A. As expected, analysis of the released carbohydrate portion by HPAEC, ESI FT-ICR MS/MS, and ^{1}H NMR spectroscopy (data not shown) indicated the presence of two compounds, Kdo and a Glc → Kdo disaccharide. MALDI-TOF mass spectrum of lipid A showed the presence of two major ion peaks at *m/z* 1798.63 (M_{LA}^{I}) and 1826.64 (M_{LA}^{II})

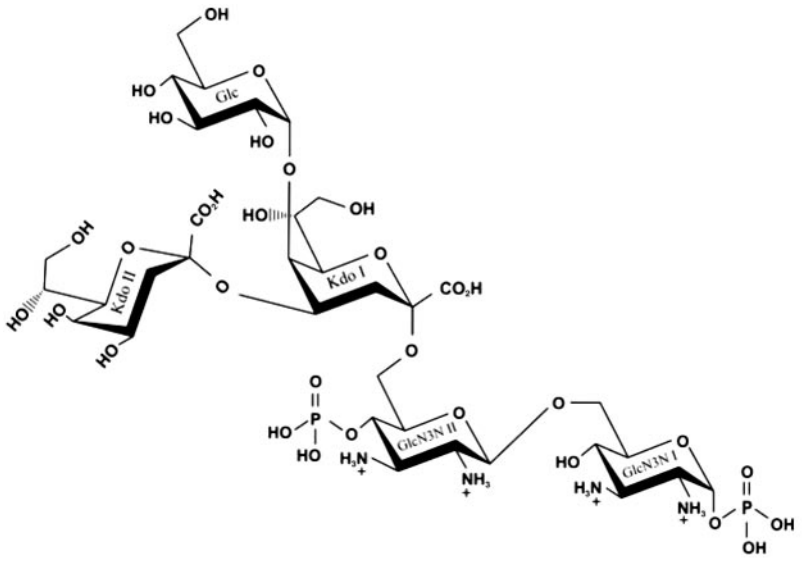

FIG. 5. **Structure of the compound 1 isolated from LPS of *B. henselae* ATCC 49882^T by stepwise *O*- and *N*-deacylation.**

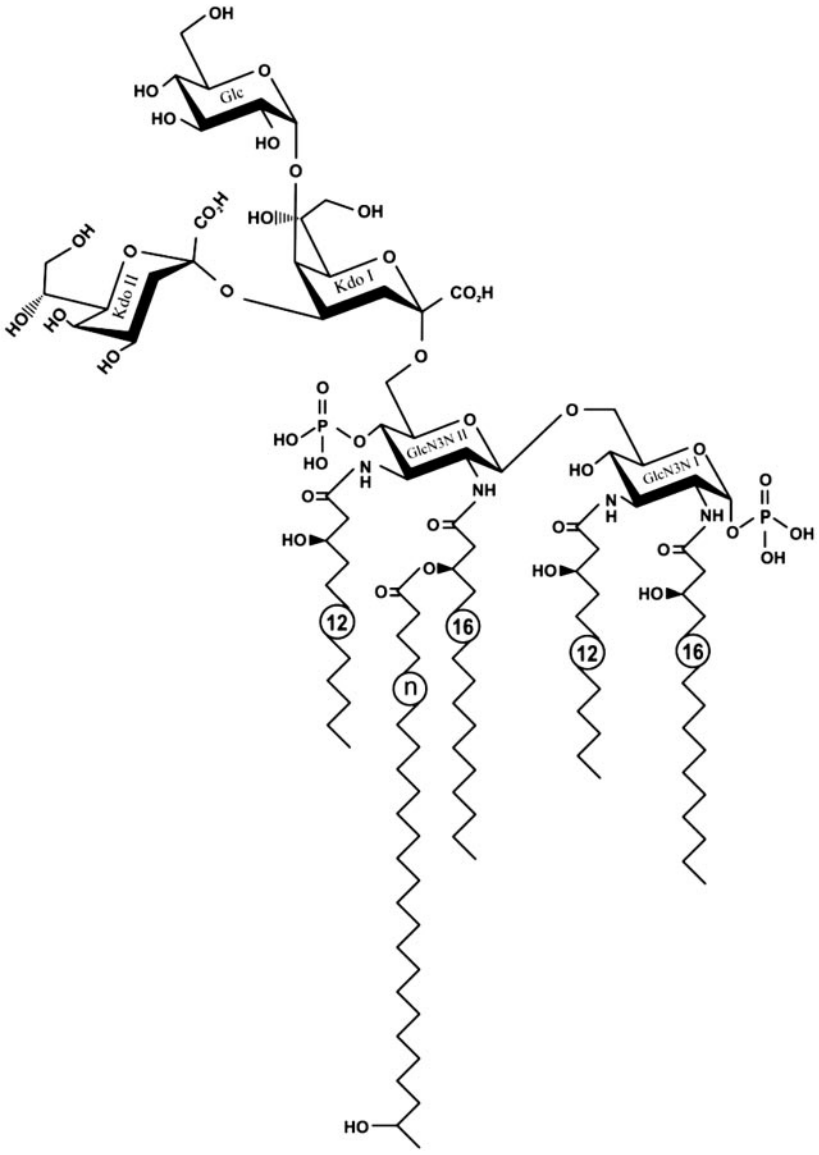

FIG. 6. **Proposed structure of two major LPS species of *B. henselae* ATCC 49882^T.** The position of 12:0(3-OH) and 16:0(3-OH) within each GlcN3N residue could be interchanged; 26:0(25-OH) and 28:0(27-OH) (n = 26 and 28, respectively) could be attached to either 16:0(3-OH), as shown, or 12:0(3-OH) on GlcN3N^{II}. Minor LPS species may differ in the replacement of 12:0(3-OH) with 12:1(3-OH) or 14:0(3-OH) and/or 16:0(3-OH) with 18:0(3-OH) or 18:1(3-OH).

in similar amounts. They corresponded to bisphosphorylpentaacyl lipid A species containing two residues each of 12:0(3-OH) and 16:0(3-OH) and one residue of 26:0(25-OH) or 28:0(27-OH), respectively. These data were in full agreement with the data obtained on the whole LPS. Minor ion peaks were also present, which could be assigned to (i) the corresponding tet-

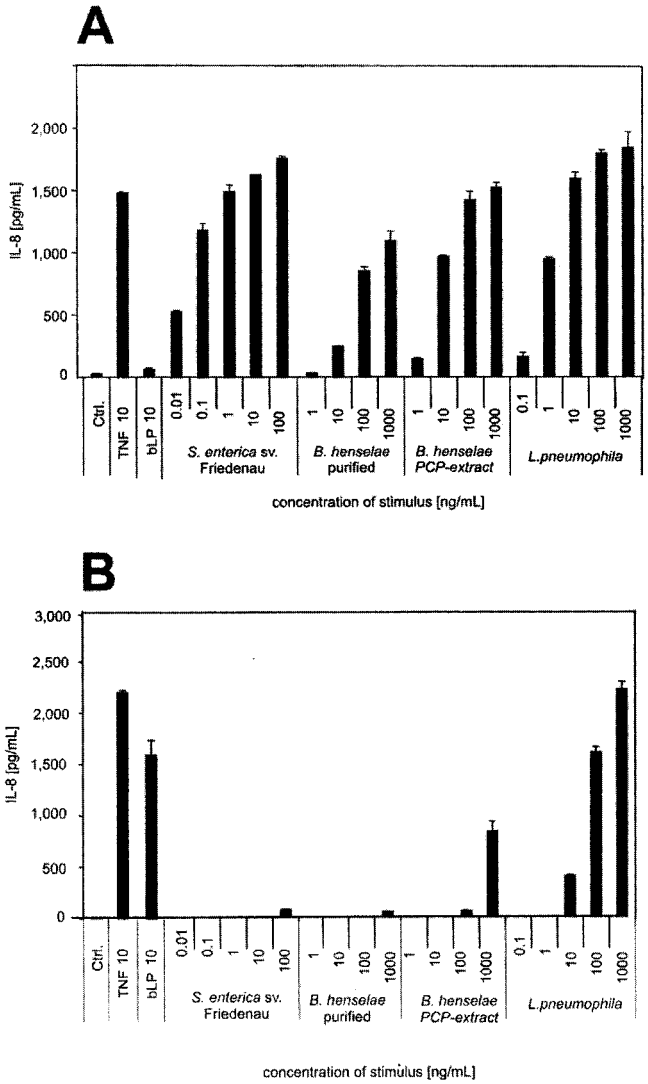

FIG. 7. **Purified LPS from *B. henselae* ATCC 49882^T activates HEK293 cells through TLR-4/MD-2.** HEK293 cells were transiently transfected with CD14 and either TLR4/MD-2 (*A*) or TLR2 (*B*) as described under "Experimental Procedures." After 24 h, cells were stimulated with indicated ligands for 18 h. Interleukin-8 content of the supernatant was analyzed by enzyme-linked immunosorbent assay. One representative experiment out of three is shown.

raacyl species lacking 26:0(25-OH) and 28:0(27-OH) (M_{LA}^{I} − 394 or M_{LA}^{II} − 422), (ii) the species with longer-chain fatty acids (M_{LA} + 28), *e.g.* those containing 14:0(3-OH) or 18:0(3-OH) instead of 12:0(3-OH) or 16:0(3-OH), respectively, and (iii) monophosphoryl species (M_{LA} − 80). No tetraacyl and no monophosphoryl lipid A species could be detected in studies of the whole LPS, and, hence, they were produced during mild acid degradation of LPS.

These data together showed that the short-chain LPS of *B. henselae* ATCC 49882^T has the structure shown in Fig. 6.

TLR2 and TLR4/MD-2-dependent Activity in HEK293 Cells—Next, we investigated which receptors are involved in the activation of cells by LPS from *B. henselae* and *Legionella pneumophila* having a similar lipid A structure (32). HEK293 cells were transiently transfected with CD14 and either TLR2 or TLR4/MD-2 and stimulated with various LPS preparations. As shown in Fig. 7, the LPS preparations from *S. enterica* sv. Friedenau, *L. pneumophila*, and *B. henselae* all showed TLR4 activity, although to a different extent. In comparison to the standard LPS preparation from *S. enterica* sv. Friedenau, *B. henselae* LPS appears to be at least 1,000-fold less active with respect to TLR4 activity. *L. pneumophila* LPS expressed a slightly higher TLR4 activity, still being 10–100-fold less than that of *S. enterica* sv. Friedenau LPS (Fig. 7*A*).

In contrast to TLR4, TLR2 activity was stimulated only by the crude LPS extracts from *L. pneumophila* and *B. henselae* but neither by the purified *B. henselae* LPS nor by that of *S. enterica* sv. Friedenau (Fig. 7*B*). The *L. pneumophila* LPS preparation showed strong TLR2 activity already at 10 ng/ml, which reached at 100 ng/ml a level comparable with the standard bacterial lipopeptide (Pam_3CysSK_4) preparation serving as positive control. The absence of CD14 in TLR2 as well as TLR4/MD-2 transfected cells reduced the activity of all tested LPS preparations but did not alter the observed differences in their activity (data not shown).

DISCUSSION

In this study, we have determined the molecular structure and biological, *i.e.* endotoxic activity of the major short-chain LPS form *B. henselae* ATCC 49882^T. This represents the first detailed LPS structure analysis of a member of the expanding genus *Bartonella*, which currently comprises 19 species of facultative intracellular pathogens, including eight species associated with human diseases (4).

The lipid A backbone of *B. henselae* ATCC 49882^T is composed of a bisphosphorylated GlcN3N disaccharide shared with only a few bacteria, including *Pseudomonas diminuta*, *Bradyrhizobium japonicum* (29), and *L. pneumophila* (32). Lipid A of *Campylobacter jejuni*, which is thus far the most thoroughly investigated representative of a GlcN3N-containing lipid A, is composed predominately of a hybrid GlcN3N-GlcN disaccharide, whereas GlcN3N-GlcN3N is found in minor LPS species (24). The GlcN3N-containing lipid A of *C. jejuni* has apparently similar endotoxic activities as those with the typical GlcN-containing backbone. Thus, there are so far no indications that the replacement of GlcN with GlcN3N in the lipid A backbone of *C. jejuni* influences its biological and physicochemical behavior (24, 33).

However, recently it has been reported that the LPS or lipid A from *L. pneumophila* can bind to and signal via TLR2 (34). The same TLR2-dependent signaling was observed for *Leptospira interrogans* LPS (35). As both lipid A's share an identical 4′-*P*-β-D-Glc*p*N3N-(1→6)-α-D-Glc*p*N3N-(1→*P* sugar backbone (36), we were curious to find out whether this structural feature might determine TLR2 *versus* TLR4 specific signaling. Since the LPS of *B. henselae* shares the same GlcN3N-GlcN3N-containing lipid A backbone, we examined whether the LPS of *B. henselae* can activate TLR2 signaling to a similar extend as *L. pneumophila* and *L. interrogans* LPS. We found that, in contrast to *L. pneumophila* LPS, the purified, protein-free LPS from *B. henselae* did not mediate any considerable TLR2 activation when tested in transiently transfected HEK cells. In agreement with what is stated above on the *C. jejuni* LPS, we thus conclude that the nature of the monosaccharide constituents in the lipid A backbone (GlcN *versus* GlcN3N) may not be critical for the endotoxic activity nor determines this structural feature TLR2-specific signaling.

The *B. henselae* lipid A is pentaacylated with each GlcN3N unit carrying one residue each of 3-hydroxydodecanoic and 3-hydroxyhexadecanoic acid. In addition, the non-reducing GlcN3N II residue carries one ester-linked long-chain fatty acid, which is either 25-hydroxypentacosanoic acid (26:0(25-OH)) or 27-hydroxyheptacosanoic acid (28:0(27-OH)). All *Rhizobiaceae* (*i.e.* the plant symbiontic rhizobia) and a few other *Rhizobiales,* including intracellular mammalian pathogens *Bartonella* and *Brucella*, examined to date contain a (ω-1)-hydroxylated long-chain fatty acids in their lipid A, likely reflecting their phylogenetic relationship (11, 29). However, be-

cause of a limited number of detailed structural studies on lipid A's from these organisms, and because of difficulties associated with analyzing the long-chain fatty acids, the location, stoichiometry, and type of attachment of these substituents is known only for a few species, including *Sinorhizobium* sp. NGR234 and *R. etli-R. leguminosarum* (30, 31). Interestingly, LPS of the unrelated intracellular pathogen *L. pneumophila* appears to have a related structure too (32) with similar long-chain fatty acids. However, *L. pneumophila* lipid A differs in the (ω-1)-substituent, which is either 28:0(27-keto) or 27:0(dioic) acid. In addition, *L. pneumophila* and *B. henselae* differ in the degree of lipid A acylation, *B. henselae* having a pentaacyl lipid A and *L. pneumophila* a hexaacyl lipid A (32).

These common structural features of LPS found among intracellular plant symbionts (*i.e.* the bacteroids of rhizobia) and intracellular mammalian pathogens *B. henselae* and *L. pneumophila* are expected to have implications for their biological activity. It is well known that enterobacterial lipid A with a reduced number of fatty acids, such as a pentaacyl lipid A lacking a secondary myristic acid (14:0) residue in *waaN*-mutant of *S. enterica* sv. Typhimurium, expresses significantly lower endotoxic activities in mouse peritoneal model (38). These *in vivo* data are in full agreement with previous results showing that the acylation pattern significantly influences the endotoxic activity in macrophages in various *in vitro* test systems (24, 33). In addition, it was postulated (32, 37) that long-chain fatty acids, as they are present in *L. pneumophila,* might be responsible for the failure to interact with CD14 and TLR4 (37). *B. henselae* lipid A possesses both features known to reduce endotoxicity, including a pentaacyl lipid A and a long-chain fatty acid. Consequently, it showed an at least 1,000-fold lower activity for signaling via TLR4 as compared with LPS from enteric bacteria, *e.g.* that from *S. enterica* sv. Friedenau. Similar to enterobacterial LPS, TLR4-mediated signaling by *B. henselae* LPS is CD14-dependent. It remains to be demonstrated whether the low endotoxic activity of *B. henselae* LPS results from a diminished interaction with CD14, with TLR4 or with both receptors.

In contrast to the TLR2 activity of *L. pneumophila* LPS (34), we could almost completely eliminate the TLR2 activity of *B. henselae* LPS upon further purification, especially with reduction of contaminating protein. The reason for the different TLR-specificity of the structurally related LPS from *L. pneumophila* and *B. henselae* remains elusive. As outlined above, the only difference in lipid A's of the two bacteria lies in the nature and number of fatty acids. In *L. pneumophila,* the main lipid A species carries six acyl groups, including *iso*- and dihydroxy-atty acids (*e.g. i*14:0(2,3-diOH)) and 28:0(27-keto) or 27:0(dioic) long-chain fatty acids (32). In contrast, *B. henselae* lipid A carries five acyl groups, no *iso*- and dihydroxy fatty acids, and 26:0(25-OH) or 28:0(27-OH) long-chain fatty acids. The importance of the number and the nature of acyl residues with respect to TLR2 and TLR4 signaling specificity is further supported with an example of lipid A's from *Porphyromonas gingivalis* (39) and *L. interrogans* (35, 36), which do not share any special structural relationship to each other in their acylation pattern. However, like *L. pneumophila,* they express TLR2--dependent rather than TLR4-dependent activity. Since *B. henselae* has a pentaacyl lipid A these data indicate that neither the structure of the lipid A backbone nor the degree of phosphorylation or acylation are sufficient to determine TLR2- and TLR4-specific activity. However, the fatty acid composition (*i.e.* the presence of hydroxy, olefinic, keto, and dihydroxy groups) represent distinct structural motifs of these lipid A and may thus contribute to determining TLR2 *versus* TLR4 specificity.

The carbohydrate portion of *B. henselae* rough-type LPS was found to consist of a branched trisaccharide, containing a glucose residue attached at position 5 of an α-(2→4)-linked Kdo disaccharide. A terminal Glc and the absence of L-*glycero*-d-*manno*-heptose and mannose (Man) (40) are remarkable features of this short-chain LPS core. While carbohydrate structures of a similar size are typically present in LPS of deep-rough mutants of bacteria otherwise containing O-polysaccharide chains, all isolates of the obligate intracellular pathogen *C. trachomatis* investigated so far contain an unbranched Kdo trisaccharide (41). Given the obligate intracellular life style of *C. trachomatis*, the short-chain carbohydrate moiety of LPS might help adaptation of the bacterium to intracellular life. The R-form LPS of the facultative intracellular pathogen *B. henselae* does not seem to result from a deep-rough mutation as at least one minor S-form LPS species is simultaneously produced in ATCC 49882^T and all other tested isolates (12). Heterogeneity of LPS in regard to the presence of an *O*-chain has previously been reported for the closely related species *B. bacilliformis* (14) and *B. quintana*,[2] as well as for some other rhizobacteria, including the plant symbionts *Bradyrhizobium japonicum* (28) and *Sinorhizobium* sp. NGR234 (31), and may be a typical feature of the *Rhizobiales*. Interestingly, synthesis of the LPS *O*-chain in *Sinorhizobium* sp. NGR234 is regulated differently in the free-living *versus* endosymbiotic state (31), suggesting that the relative proportion of R-form to S-form LPS species may be a critical factor for the facultative intracellular life style of this plant symbiont. In future it will be interesting to recognize whether the facultative intracellular pathogen *B. henselae* can regulate synthesis of different amounts of R-form *versus* S-form LPS species in response to environmental signals as a specific adaptation to the host.

Acknowledgments—We thank M. Röttgen for helpful discussions. We acknowledge H. P. Cordes, L. Brecker, and H. Lüthje for help with NMR and MALDI-TOF mass spectroscopy; K. Jakob and I. Goroncy for technical assistance; and H. Moll for expert GC-MS analysis. Dr. Yves Piemont is acknowledged for providing strain ISB 113. We thank Henri Saenz for critical reading of the manuscript.

REFERENCES

1. Dehio, C. (2001) *Trends Microbiol.* **9,** 279–285
2. Karem, K. L., Paddock, C. D., and Regnery, R. L. (2000) *Microbes Infect.* **2,** 1193–1205
3. Dehio, C., Meyer, M., Berger, J., Schwarz, H., and Lanz, C. (1997) *J. Cell Sci.* **110,** 2141–2154
4. Dehio, C. (2003) *Curr. Opin. Microbiol.* **6,** 61–65
5. Maeno, N., Oda, H., Yoshiie, K., Wahid, M. R., Fujimura, T., and Matayoshi, S. (1999) *Microb. Pathog.* **27,** 419–427
6. Kirby, J. E., and Nekorchuk, D. M. (2002) *Proc. Natl. Acad. Sci. U. S. A.* **99,** 4656–4661
7. Resto-Ruiz, S. I., Schmiederer, M., Sweger, D., Newton, C., Klein, T. W., Friedman, H., and Anderson, B. E. (2002) *Infect. Immun.* **70,** 4564–4570
8. Erridge, C., Bennett-Guerrero, E., and Poxton, I. R. (2002) *Microbes Infect.* **4,** 837–851
9. Faure, E., Equils, O., Sieling, P. A., Thomas, L., Zhang, F. X., Kirschning, C. J., Polentarutti, N., Muzio, M., and Arditi, M. (2000) *J. Biol. Chem.* **275,** 11058–11063
10. Fuhrmann, O., Arvand, M., Gohler, A., Schmid, M., Krull, M., Hippenstiel, S., Seybold, J., Dehio, C., and Suttorp, N. (2001) *Infect. Immun.* **69,** 5088–5097
11. Schmid, M. C., Schulein, R., Dehio, M., Denecker, G., Carena, I., and Dehio, C. (2004) *Mol. Microbiol.* **52,** 81–92
12. Kyme, P., Dillon, B., and Iredell, J. (2003) *Microbiology* **149,** 621–629
13. Bhat, U. R., Carlson, R. W., Busch, M., and Mayer, H. (1991) *Int. J. Syst. Bacteriol.* **41,** 213–217
14. Minnick, M. F. (1994) *Infect. Immun.* **62,** 2644–2648
15. Liberto, M. C., and Matera, G. (2000) *Microbiologica* **13,** 449–456
16. Liberto, M. C., Matera, G., Lamberti, A. G., Barreca, G. S., Quirino, A., and Foca, A. (2003) *Diagn. Microbiol. Infect. Dis.* **45,** 107–115
17. van den Akker, W. M. R. (1998) *Microbiology* **144,** 1527–1535
18. Westphal, O., and Jann, K. (1965) *Methods Carbohydr. Chem.* **5,** 83–91
19. Galanos, C., Luderitz, O., and Westphal, O. (1969) *Eur. J. Biochem.* **9,** 245–249
20. Hirschfeld, M., Weis, J. H., Vogel, S., and Weis, J. J. (2000) *J. Immunol.* **165,** 618–622
21. Sawardeker, J. S., Sloneker, J. H., and Jeanes, A. (1965) *Anal. Chem.* **37,** 1602–1605

[2] U. Zähringer, B. Lindner, Y. A. Knirel, W. M. R. van den Akker, R. Hiestand, H. Heine, and C. Dehio, unpublished data.

22. Sonesson, A., Moll, H., Jantzen, E., and Zähringer, U. (1993) *FEMS Microbiol. Lett.* **106,** 315–320
23. Ciucanu, I., and Kerek, F. (1984) *Carbohydr. Res.* **131,** 209–217
24. Zähringer, U., Lindner, B., and Rietschel, E. T. (1994) *Adv. Carbohydr. Chem. Biochem.* **50,** 211–276
25. Knirel, Y. A., Helbig, J. H., and Zähringer, U. (1996) *Carbohydr. Res.* **283,** 129–139
26. Kosma, P., D'Souza, F. W., and Brade, H. (1995) *J. Endotoxin Res.* **2,** 63–76
27. Knirel, Y. A., Grosskurth, H., Helbig, J. H., and Zähringer, U. (1995) *Carbohydr. Res.* **279,** 215–226
28. Bock, K., Thomsen, J. U., Kosma, P., Christian, R., Holst, O., and Brade, H. (1992) *Carbohydr. Res.* **229,** 213–224
29. Carrion, M., Bhat, U. R., Reuhs, B., and Carlson, R. W. (1990) *J. Bacteriol.* **172,** 1725–1731
30. Bhat, U. R., Mayer, H., Yokota, A., Hollingsworth, R. I., and Carlson, R. W. (1991) *J. Bacteriol.* **173,** 2155–2159
31. Gudlavalleti, S. K., and Forsberg, L. S. (2003) *J. Biol. Chem.* **278,** 3957–3968
32. Zähringer, U., Knirel, Y. A., Lindner, B., Helbig, J. H., Sonesson, A., Marre, R., and Rietschel, E. T. (1995) *Prog. Clin. Biol. Res.* **392,** 113–139
33. Rietschel, E. T., Kirikae, T., Schade, F. U., Mamat, U., Schmidt, G., Loppnow, H., Ulmer, A. J., Zähringer, U., Seydel, U., Di Padova, F., Schreier, M. H., and Brade, H. (1994) *FASEB J.* **8,** 217–225
34. Girard, R., Pedron, T., Uematsu, S., Balloy, V., Chignard, M., Akira, S., and Chaby, R. (2003) *J. Cell Sci.* **116,** 293–302
35. Werts, C., Tapping, R. I., Mathison, J. C., Chuang, T.-H., Kravchenko, V. V., Saint Girons, I., Haake, D. A., Godowski, P. J., Hayashi, F., Ozinsky, A., Underhill, D. M., Kirschning, C. J., Wagner, H., Aderem, A., Tobias, P. S., Ulevitch, R. J. (2001) *Nature Immunol.* **2,** 346–352
36. Que, N. L. S., Ramirez, S., Werts, C., Ribeiro, A., Bulach, D., Cotter, R., and Raetz, C. R. H. (2002) *J. Endotoxin Res.* **8,** 156
37. Neumeister, B., Faigle, M., Sommer, M., Zähringer, U., Stelter, F., Witt, S., Schütt, C., and Northoff, H. (1998) *Infect. Immun.* **66,** 4151–4157
38. Khan, S. A., Everest, P., Servos, S., Foxwell, N., Zähringer, U., Brade, H., Rietschel, E. Th., Dougan, G., Charles, I. G., and Maskell, D. J. (1998) *Mol. Microbiol.* **29,** 571–579
39. Hirschfeld, M., Weis, J. J., Toshchakov, V., Salkowski, C. A., Cody, M. J., Ward, D. C., Qureshi, N., Michalek, S. M., and Vogel, S. N. (2001) *Infect. Immun.* **69,** 1477–1482
40. Holst, O. (1999) in *Endotoxin in Health and Disease* (Brade, H., Opal, S. M., Vogel, S. N., and Morrison, D. C., eds) pp. 115–154, Marcel Dekker, New York
41. Rund, S., Lindner, B., Brade, H., and Holst, O. (1999) *J. Biol. Chem.* **274,** 16819–16824